Journal of Environmental Chemical Engineering 5 (2017) 1801–1808

Contents lists available at ScienceDirect

Journal of Environmental Chemical Engineering

journal homepage: www.elsevier.com/locate/jece

Preparation of activated carbon from bamboo-cellulose fiber and its use for EDLC electrode material

Masatsugu Fujishige[a], Ichiro Yoshida[a], Yumiko Toya[a], Yasuo Banba[a], Kyo-ichi Oshida[b], Yu-suke Tanaka[c], Paweena Dulyaseree[d], Winadda Wongwiriyapan[d], Kenji Takeuchi[a,*]

[a] Institute of Carbon Science and Technology, Shinshu University, 4-17-1 Wakasato, Nagano, 380-8553, Japan
[b] Nagano National College of Technology, 716 Tokuma, Nagano, 380-8550, Japan
[c] Interdisciplinary Graduate School of Science and Technology, Shinshu University, 4-17-1 Wakasato, Nagano, 380-8553, Japan
[d] College of Nanotechnology, King Mongkut's Institute of Technology Ladkrabang, Chalongkrung Road, Ladkrabang, Bangkok 10520, Thailand

ARTICLE INFO

Article history:
Received 21 December 2016
Received in revised form 18 February 2017
Accepted 9 March 2017
Available online 11 March 2017

Keywords:
Bamboo
Cellulose fiber
Activated carbon
EDLC electrode
Carbonization

ABSTRACT

Carbonization and post activation of bamboo-cellulose fiber was carried out. The carbonization was performed at 600 °C, 800 °C and 1000 °C in argon atmosphere. Then, they were activated by heating solid mixture of carbonized bamboo and sodium hydroxide (NaOH) at 720 °C in argon atmosphere. The largest specific surface area of the resulting activated carbon (carbonized at 600 °C) was 2366 m^2/g with the micropore volume of 0.71 cm^3/g and mesopore volume of 0.06 cm^3/g. It was found that the carbonization temperature is very important to obtain nanoporous carbon with large specific surface area. The distributions of interlayer spacing were estimated from the power spectra of the TEM images of the carbonized samples. It showed the interlayer spacing of basic structural unit (BSU) decreased from 0.49 nm (BC-0600) through 0.47 nm (BC-0800) to 0.45 nm (BC-1000). The activated carbon was used as the host material of the electrodes of coin type electric double-layer capacitor (EDLC) with organic electrolyte. The observed specific capacitance was 43 F/g (23 F/cm^3) for the activated carbon (carbonized at 600 °C), comparable to 44 F/g (22 F/cm^3) of commercial activated carbon (MSP). The corresponding values for the activated carbons (carbonized at 800 °C and 1000 °C) were 40 F/g (23 F/cm^3) and 17 F/g (12 F/cm^3), respectively.

1. Introduction

A lot of carbon materials have been produced from fossil fuels such as petroleum and coal. However, it becomes interesting strongly to use bio resources instead of fossil fuels for getting the sustainable society to fruition. Bamboo is generally native to warm and moist tropical and temperate climates [1]. Bamboo has been used in Japan, since olden days, as building materials, craftworks, paper, musical instruments, charcoal, etc. However, the life changes in the times, with the increase of alternate-material from plastic and cheap imports, both production and consumption of bamboo decrease sharply in Japan [2]. Bamboo consumption was 11,091 ton in 1975, while it became 1531 ton in 2013, corresponding to 14% of that in 1975. Moreover, encroachment of forests, called "CHIKUGAI" in Japanese, has become a severe problem in Japan [3,4]. Therefore, it is very important to utilize bamboo for various industrial applications such as electrode of electric double-layer capacitor (EDLC) or lithium-ion battery.

Carbon materials have been widely used in various fields: activated carbon, carbon black, carbon fibers, electrodes in steel and aluminum industries, electrodes of lithium ion battery and EDLC (Electric Double Layer Capacitor), etc. The EDLC attracts attention because of its high rate performance and long life cycle [5]. Controlling surface area, pore size and shape of carbon materials is the key technology for increasing capacity. However, this is very difficult in fact and still challenging work. A lot of work on the carbonization and activation of bamboo has been reported [6–14]. Chen et al. reported the preparation of nitrogen and boron co-doped KOH-activated bamboo-derived carbon as supercapacitor electrode material [14]. This material exhibited the capacitance of 281 F/g in 1M-KOH and 318 F/g in 1M-H_2SO_4.

In the present investigation, we used a bamboo-cellulose fiber as the starting material. The dried bamboo-cellulose fiber was carbonized at different temperatures of 600, 800 and 1000 °C and then activated by the heat-treatment of the solid mixture of the carbonized bamboo with sodium hydroxide (NaOH) at 720 °C.

* Corresponding author.
E-mail address: takeuchi@endomoribu.shinshu-u.ac.jp (K. Takeuchi).

http://dx.doi.org/10.1016/j.jece.2017.03.011
2213-3437/

2. Experimental

2.1. Sample preparation

Aqueous slurry solution of bamboo-cellulose fiber, containing 10% in mass, was used as the starting material. The solution was then dried in an air chamber kept at 60 °C for 24 h. It was shattered by a blender with rotation velocity of 25,000 rpm (WB-1: OSAKA CHEMICAL Co., Ltd.). Thermal behavior of the dried bamboo fiber was determined by the thermogravimetric analysis (TGA) using STA7200RV (Hitachi). In this analysis, the mass of bamboo carbon (hereafter abbreviated as BC) was recorded continuously with temperature in nitrogen atmosphere, where temperature increased linearly from ambient to as high as 1000 °C with heating rate of 5 °C/min. The dried bamboo-cellulose fiber was carbonized at three different temperatures, 600, 800 and 1000 °C, in the tube furnace under argon gas flow with flow rate of 0.5 L/min. Hereafter the BC samples prepared at 600 °C, 800 °C and 1000 °C are written as BC-0600, BC-0800 and BC-1000, respectively. The activation of the BC was performed by the heat-treatment of a solid mixture of BC and NaOH (in molar ratio of 1/2.5) in the tube furnace at 720 °C under argon gas flow. The activated BC samples were similarly designated as AC-0600, AC-0800 and AC-1000, where AC is the abbreviation of activated carbon. It should be noted here that the activation temperature was fixed at 720 °C, irrespective of the carbonization temperature, because the present investigation tried to clarify the effect of carbonization temperature on the surface properties and EDLC characteristics of the resulting activated carbons. The fact that our preliminary experiment showed that the activation was fairly effectively performed at 720 °C was also taken in account for determining the activation temperature.

2.2. Characterization and electrochemical measurement of bamboo carbons and activated bamboo carbons

The morphology of BC and AC samples was observed by scanning electron microscope (SEM, JSM-7000F-JEOL) and high resolution transmission electron microscopy (TEM, 2100F-JEOL) with Cs corrector. The Raman spectra were measured by inVia Raman microscope (Renishaw) using a light with $\lambda = 532$ nm. The nitrogen-adsorption isotherms of BC and AC samples at 77 K were observed by the gas adsorption analyzers (ASAP 2020-Micromeritics). The BET surface area and pore volume were determined from the adsorption isotherms. The calculation of the pore volume was performed based on the method of the density functional theory (DFT) [15].

The AC samples were used as the host material of the electrodes of coin type EDLC. The AC samples were mixed with polytetrafluoroethylene (5% in mass) and carbon black (5% in mass). The electrolyte was tetraethylammonium tetrafluoroborate (Et_4NBF_4) dissolved in propylene carbonate. The concentration of Et_4NBF_4 in the solution was adjusted to be 1 mol/L. The capacitance of the EDLC was calculated from the charge and discharge curves.

3. Results and discussions

3.1. Characterization of bamboo carbons and activated carbons

A significant weight change was observed at around 335 °C. The carbonization yield of BC at 1000 °C was estimated to be approximately 23%. Similar observations are reported: More than 70% weight loss was observed at around 350 °C for Indian bamboo [16] and 68 ~ 72% weight loss was observed between 600 °C and 1000 °C for Moso-bamboo [8]. This means that BC can be produced at fairly low temperature such as 600 °C. It is also reported that for bamboo carbonization, the aromatization of residual carbon is approximately completed at 600 °C [17]. Based on these findings, we carbonized the bamboo-cellulose fiber at 600 °C, 800 °C and 1000 °C to examine the effect of carbonization temperature on the electrochemical behavior of BC.

The SEM images of the bamboo carbons (BC-0600, BC-0800 and BC-1000) are shown in Fig. 1. Although the starting fibrous structure of cellulose fiber remains a little bit, they fused each other; the degree of the fusion develops with increasing carbonization temperature. It suggests that the destruction and coagulation of the bamboo-cellulose fibers take place during carbonization process. The destruction and coagulation process was also suggested by FT-IR observation. Fig. 2 shows the FT-IR spectra of starting bamboo cellulose-fiber and BC-0600, BC-0800 and BC-1000. The spectra of carbonized samples are very similar. By the carbonization, the intensities of wide-band absorption at around 3400 cm^{-1} (hydroxyl or carboxyl), the peak at 2900 cm^{-1} (aliphatic methylene) and the peak at 1600 cm^{-1} (C=C, benzene ring skeleton) were reduced. The feature is in agreement with the observation in the carbonization of cellulose, which suggests that the benzene rings of the sample get closer to each other, and the

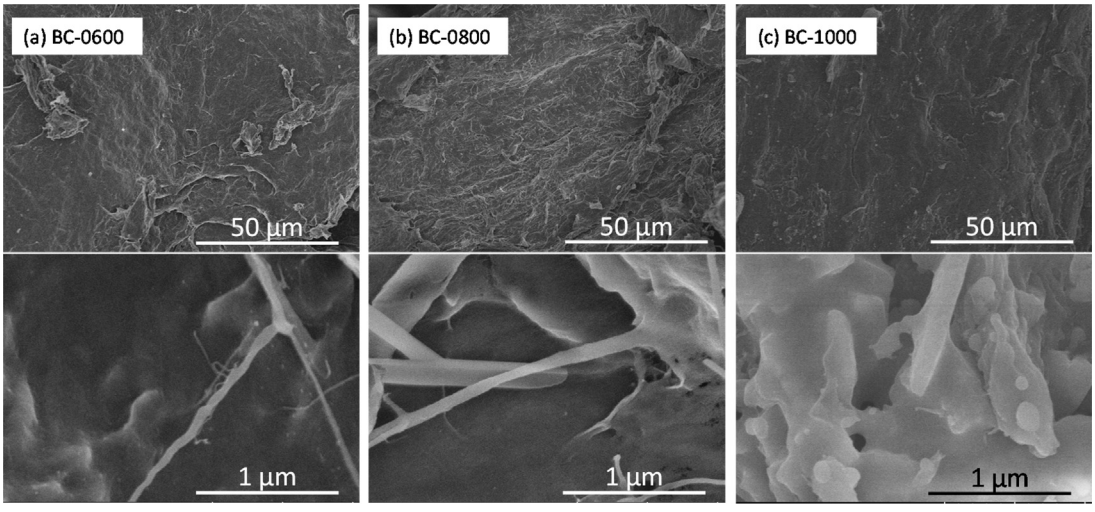

Fig. 1. SEM images of (a) BC-0600, (b) BC-0800 and (c) BC-1000.

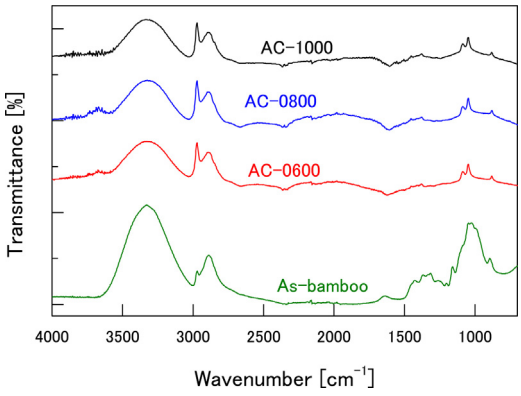

Fig. 2. FT-IR spectra of starting bamboo cellulose-fiber and BC-0600, BC-0800 and BC-1000.

benzene fused-ring structure is formed [18]. Their TEM images of BC (Fig. 3(a)–(c)) and AC (Fig. 3(g)–(i)) are characteristic of that of amorphous carbon, being composed of short length of hexagonal carbon layers. In Fig. 2(a), two or three stacks of the layers with a length of around 1 nm are observed here and there. Even with carbon considered to be amorphous, basic structural units (BSUs) exist [19]. From the TEM images of BC (Fig. 3(a)–(c)), it can be considered that the length of the hexagonal carbon layers tends to increase with the increase of the carbonization temperature. It was also observed that the spaces among the stacks of hexagonal carbon layers increased with increase of the carbonization temperature. The growth of spaces is considered to form the pore structure. The power-spectra images (insets of Fig. 3(d)–(f)) were obtained by 2 dimensional fast Fourier transform (2D-FFT) on the TEM images of Fig. 3(a)–(c). The distributions of interlayer spacing were also obtained by integration along rotation-axis of power spectra [20,21]. It is clearly observed that the spacing at the peak top decreases from 0.49 nm (BC-0600) through 0.47 nm (BC-0800) to 0.45 nm (BC-1000). The spacing can be considered to be the

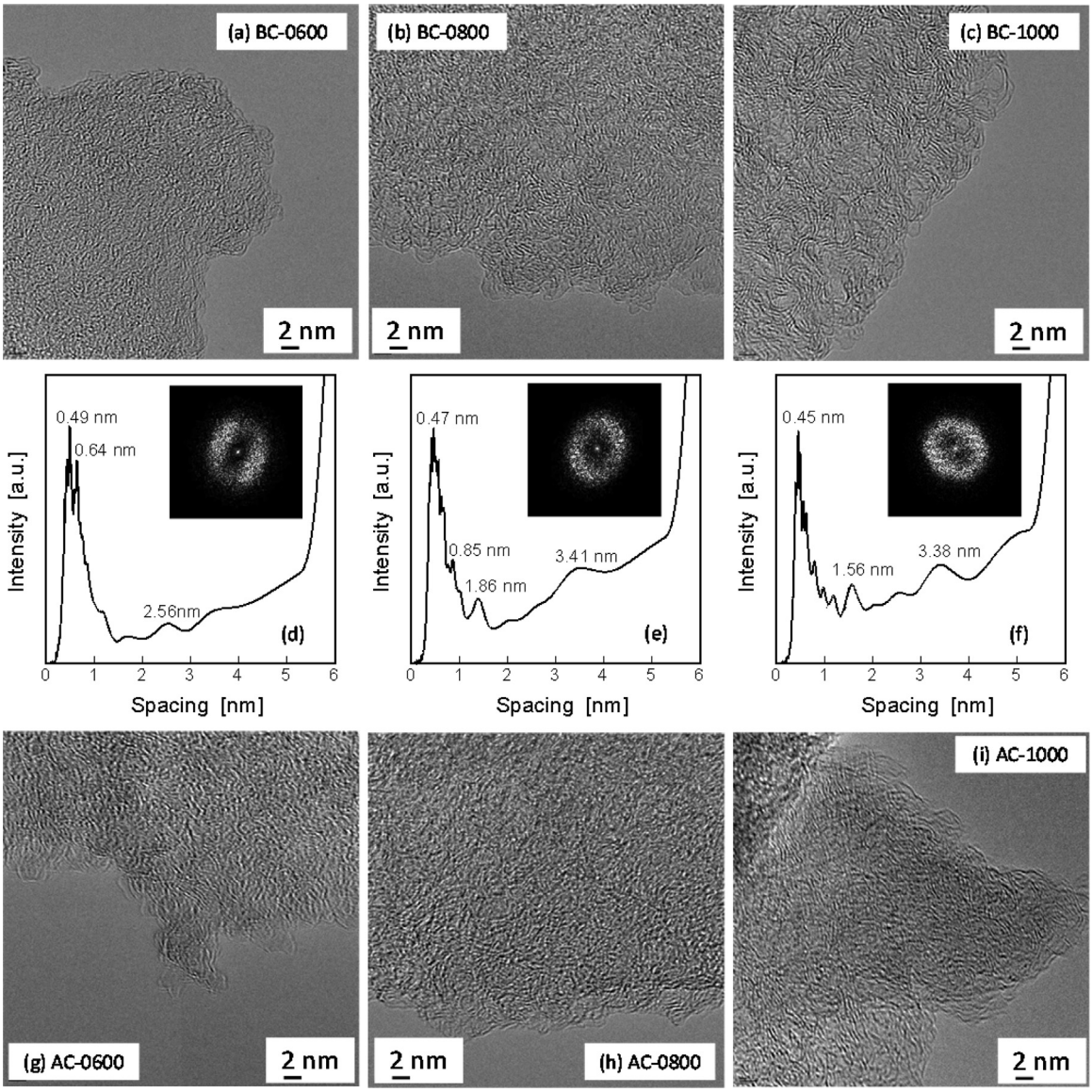

Fig. 3. TEM images, power spectra (inset) and spacing distributions of BC and AC samples: (a)–(c), TEM images of BC; (d)–(f), power spectra (inset) and spacing distributions of BC; (g)–(i), TEM images of AC.

carbon-carbon interlayer spacing. The values are large in comparison with 0.3354 nm of the interlayer distance of graphite crystal. This is because the carbonization was carried out at 600–1000 °C which is lower than graphitization temperature (higher than 1500 °C). The trend that the interlayer distance decreases with increasing carbonization temperature indicates the advance of the structural regularity towards organized carbon nanosheet [22]. It is also seen in Fig. 3(d)–(f) that the broadness of the peak decreases with increasing carbonization temperature. This is the indication of the development of carbon network. The peak at 2.6 nm observed for BC-0600 is fairly small compared with 3.4 nm for BC-0800 and BC-1000. These peaks are considered to be due to area like the hole. On the other hand, the TEM images of AC (Fig. 3(g)–(i)) show the random structure irrespective of the carbonization temperature. It suggests that chemical reaction during activation attacked, to a considerable extent, the surface of carbon network.

Fig. 4 shows the Raman spectra of (a) BC-0600, BC-0800 and BC-1000, and (b) AC-0600, AC-0800 and AC-1000. All the carbon samples exhibit two broad overlapping bands at around 1360 (D band) and 1600 (G band) cm^{-1}. The spectra are typical of less graphitized carbons [23–26]. Table 1 summarizes the Raman shift (G band), FWHM (G band) and G/D ratio observed for BC and AC samples. Comparison of these data reveals that BC-0600 has smaller values of Raman shift and FWHM, in addition to larger G/D ratio as compared to AC-0600. Although this trend is similarly seen for the other couples (BC-0800/AC-0800 and BC-1000/AC-1000), except the data of FWHM, it is most clearly seen for BC-0600/AC-0600. Therefore, it can be said that the structure of BC-0600 was remarkably modified by the activation process. It is possible because BC-0600 contains a lot of structural defects (large interlayer spacing, short length of the carbon network, etc.) compared to the other ones and therefore is considered to be highly reactive against activation agent. It should be noted that potassium hydroxide (KOH) is generally used for the activation of carbons [27]. However, there are examples that NaOH activation is also effective or better for carbons derived from mangifera indica seed (Mango) [28], coconut residue [29], etc. The present investigation also confirmed that NaOH activation is useful for obtaining nanoporous carbons with large specific surface area and micro-pore volume, as will be noted bellow.

Fig. 5 shows the nitrogen adsorption-desorption isotherms of (a) BC and (b) AC samples at 77 K. The hysteresis was observed for BC samples; it implies that there are slit type pores and a space between the stacked carbon layers [30]. On the contrary, the majority of nitrogen was adsorbed at remarkably low pressure (P/P_0), and then the adsorption curve was almost flat against pressure up to saturation for AC samples. In addition, almost no hysteresis was observed for AC samples. The isotherms of the AC samples are classified to the type I (definition of IUPAC [30]). This isotherm type is given by microporous solids having relatively small external surfaces. Confirmed limiting uptake is governed by the accessible micropore volume rather than by the internal surface area. The saturated adsorbed amount of AC samples is larger than that of BC samples. This is considered to be due to the pore formation during activation process, as is usually observed. The pore size distribution for the BC and AC samples obtained by the DFT method is shown in Fig. 6. It can be seen that the AC-0600 sample have pore sizes mainly in the range of 0.5–2.5 nm. For AC-0800 and AC-1000, the pore is mainly consisted of micropore (less than 2 nm). In contrast, pore volume of BC sample was much smaller than that of AC sample, irrespective of the carbonization temperature. The specific surface area and pore volume are listed in Table 2, where the corresponding data of commercial activated carbon, MSP (Kansai Coke and Chemicals Company), is also shown. Both the specific surface area (S_{BET}) and pore volume (V_{total}) is the largest for BC-0800 among BC samples. However, AC-0600 has very large values of S_{BET} and V_{total}, comparable to those of commercial MSP. The ratio of S_{BET} (AC-0600) to S_{BET} (BC-0600) is 6.1, which is remarkably larger than the other. Although the ratio of the specific surface area of BC-0600 to BC-0800 is about 0.84, the ratio of the specific surface area of AC-600 to AC-800 is 1.38 (The ratio of the specific surface area of AC-600 to AC-1000 is 1.99). Therefore, it can be said that the effective activation was performed on BC-0600, in comparison with BC-0800 and BC-1000. It is reported that in the activation of anthracite and heat-treated anthracite with hydroxides (NaOH and KOH), the BET surface area decreased with increasing heat-treatment temperature of anthracite [31]. The

Table 1
Raman shift (G band), FWHM (G band) and G/D ratio of BC and AC.

	G band Center	G band FWHM	G/D ratio
BC-0600	1593.1	64.5	0.97
BC-0800	1596.2	69.4	0.80
BC-1000	1602.5	75.1	0.73
AC-0600	1606.7	75.6	0.59
AC-0800	1607.7	67.9	0.70
AC-1000	1605.9	65.2	0.71

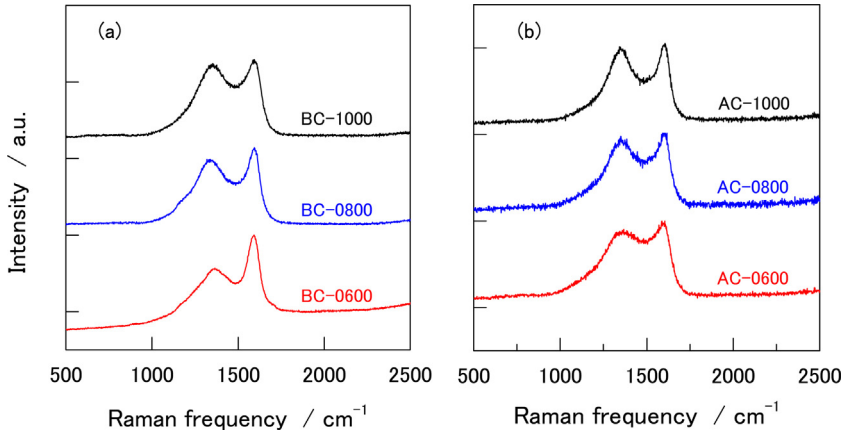

Fig. 4. Raman spectra of (a) BC and (b) AC samples.

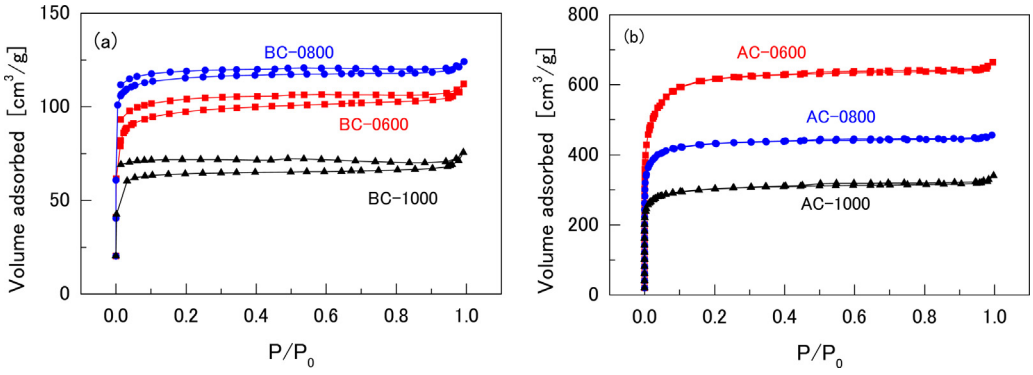

Fig. 5. Nitrogen adsorption-desorption isotherms (77 K) of (a) BC and (b) AC samples.

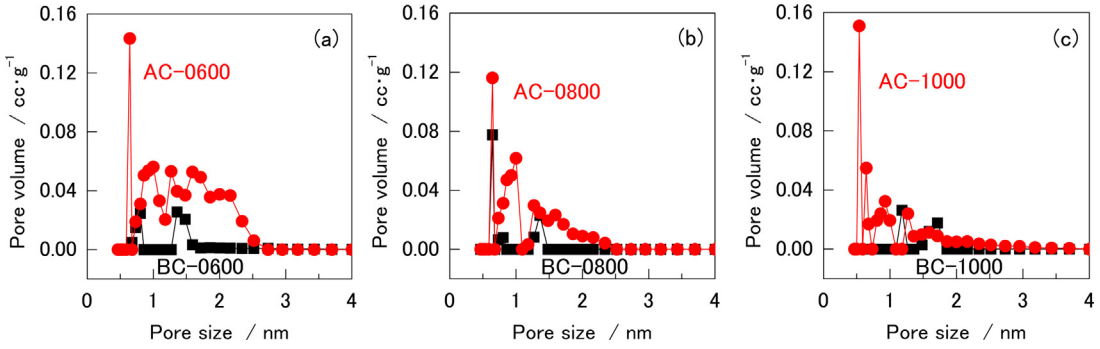

Fig. 6. Pore Size Distribution of (a) BC-0600, AC-0600, (b) BC-0800, AC-0800, and (c) BC-1000, AC-1000 calculated by the DFT method.

heat-treatment prior to activation reduces considerably the ease of the reaction. The present result shows the similar trends; the specific surface area decreased in the order of AC-0600, AC-0800 and AC-1000.

The surface properties of the nanoporous carbon derived from bamboo-cellulose fiber is compared with the reported data of carbonized and activated bamboo carbons in Table 3. The present nanoporous carbon derived from bamboo-cellulose fiber has large specific surface area and micro-pore volume. Thus, the carbonization temperature is very important to obtain nanoporous carbons with large specific surface area. Since the low-temperature carbonization at around 600 °C seems interesting, detailed study concerning the relationship between the carbonization temperature and the surface properties of the activated carbon should be carried out in near future.

3.2. EDLC characteristics of nanoporous carbon derived from bamboo-cellulose fiber

Fig. 7 shows the double layer capacitance plotted as a function of current density, where the capacity is expressed in different unit ((a) F/g and (b) F/cm^3). Reflecting the magnitude of the specific surface area, the capacitance increased in the following order: AC-1000, AC-0800 and AC-0600. The capacitance of AC-0600 (43 F/g (23 F/cm^3)) is comparable to that of MSP (44 F/g (22 F/cm^3)). The corresponding values for the activated carbons (carbonized at 800 °C and 1000 °C) were 40 F/g (23 F/cm^3) and 17 F/g (12 F/cm^3),

Table 2
Specific surface area, pore volume of BC and AC calculated from N_2 adsorption/desorption isotherms.

Sample	S_{BET}[a] [m^2/g]	V_{total}[b] [cm^3/g]	V_{micro}[c] [cm^3/g]	V_{meso}[d] [cm^3/g]	V_{macro}[e] [cm^3/g]	V_{micro}/V_{total} [%]	S_{BET}(AC)/S_{BET}(BC)
BC-0600	388	0.146	0.096	0.074	0.037	66	–
BC-0800	461	0.154	0.123	0.002	0.029	80	–
BC-1000	272	0.099	0.059	0.005	0.035	60	–
AC-0600	2366	0.810	0.712	0.064	0.034	88	6.1
AC-0800	1709	0.576	0.464	0.015	0.097	81	3.7
AC-1000	1188	0.448	0.391	0.025	0.032	87	4.4
MSP	2543	0.908	0.820	0.080	0.008	90	–

[a] BET specific surface area.
[b] DFT total pore volume.
[c] DFT micro-pore volume.
[d] DFT meso-pore volume.
[e] DFT macro-pore volume.

Table 3
Specific surface area (S_{BET}), pore volume (V_{total}) and micropore-volume ratio (V_{micro}/V_{total}) of nanoporous carbons prepared from bamboo.

Starting material	Preparation method	S_{BET} (m^2/g)	V_{total} (ml/g)	V_{micro}/V_{total} (%)	published year [Ref. No.]
Moso bamboo	carbonized in nitrogen at 500 °C and activated in air at 280 °C	428	0.24	67	2011 [6]
Moso bamboo	carbonized at 800 °C and activated in nitrogen at 800 °C and 1000 °C	493	–	–	2014 [7]
Moso bamboo	carbonized in nitrogen at 1000 °C,	151	0.11	–	2014 [8]
Bamboo (Korea)	carbonized in nitrogen at 450 °C and activated with KOH at 750 °C	1092	0.26	mainly micropore	2015 [9]
Bamboo (Nigeria)	Simultaneous carbonization and activation (KOH) at 500 °C	364	–	–	2013 [10]
Bamboo (Malaysia)	1) carbonized in nitrogen at 500 °C 2) Dehydration with 98% H_2SO_4 at room temperature	1) 293 2) 508	1) V_{micro} = 0.12 2) V_{micro} = 0.21	–	2013 [11]
Bamboo (Thailand)	Simultaneous carbonization and activation (KOH) at 800 °C	1533	–	–	2011 [12]
Bamboo (Japan)	delignification ($CH_3COOH + H_2O_2$) carbonized at 800 °C in nitrogen and activated in CO_2 at 800 °C	2000	1.4	mainly micropore	2016 [13]
Bamboo (reagent)	Simultaneous carbonization and activation (KOH) at 750 °C	40	–	–	2015 [14]
Bamboo-cellulose fiber	carbonized at 600 °C in argon and activated with NaOH at 720 °C in argon	**2366**	**0.81**	**88**	This work

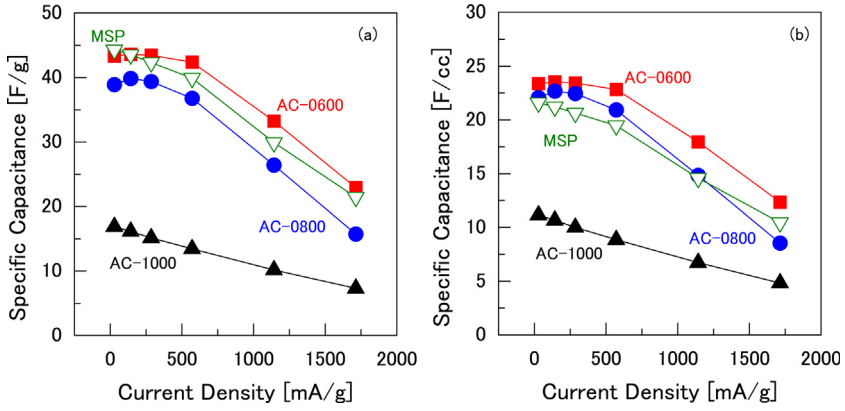

Fig. 7. Specific Capacitance plotted as a function of current density: (a), capacitance per unit mass; (b), capacitance per unit volume.

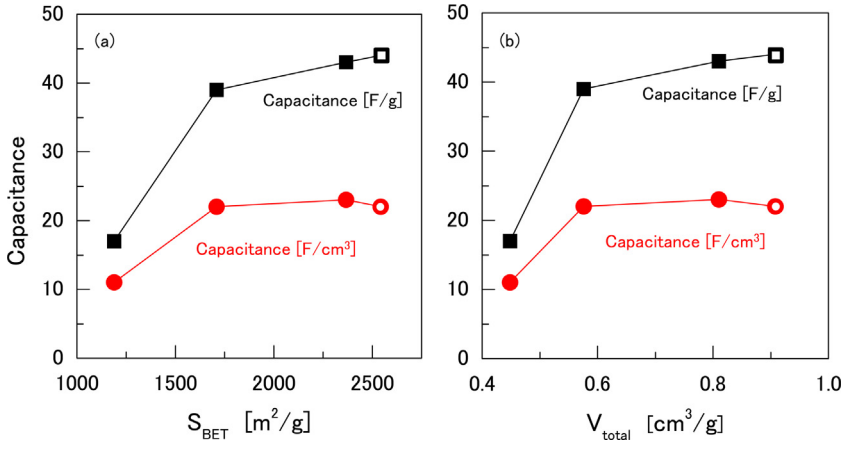

Fig. 8. Capacitance plotted vs. (a) specific surface area and (b) total volume of AC (■,●) and MSP (□,○).

respectively. These values are less than the reported capacitance for the same organic electrolyte ($TEABF_4$/PC): 65 F/g for carbon derived from melamin-mica composite material [32] and 90 F/g for carbon derived from PAN-based staple fabrics [33]. The ion size of the PC-solvated tetraethyl ammonium ion (TEA^+) and of fluoroborate ion (BF_4^-) is reported to be 1.96 nm and 1.71 nm, respectively [5]. It means that pores with the size larger than 2 nm are important for the electrode of EDLC. The capacitance is plotted as a function of specific surface area in Fig. 8(a) and also plotted against total pore volume in Fig. 8(b). The capacitance increases monotonically with increasing specific surface area in the region between 1200 m^2/g and 2500 m^2/g. At the same time, the capacitance increases with increasing total pore volume in the region between 0.45 and 0.81 cm^3/g. It is interesting to note that the ratio of micropore volume to total volume is 0.81–0.87 for the AC samples. It seems inconsistent to the above consideration that pore size should be larger than 2 nm. The mesopore (2–50 nm) volume in Table 2, however, cannot explain the observed capacitance. In the diagram of the pore-size distribution (Fig. 6) a fairly large population is seen in the range 2.0–2.5 nm for AC-0600; it decreases in the order of AC-0600, AC-0800, AC-1000. If the population of this range correlates with micropore volume, the relation between capacitance and micropore volume can be understood. It will be interesting to examine the relation between the EDLC capacity and the number of pores with diameter in the range 2.0–2.5 nm.

4. Conclusions

Nanoporous carbon was prepared by the carbonization of bamboo-cellulose fiber at different temperatures of 600 °C, 800 °C 1000 °C, and the succeeding activation by sodium hydroxide at 720 °C. It was found that the carbonization temperature was very important for obtaining nanoporous carbon with large specific surface area. The present investigation showed that the carbonization at 600 °C was the best. It is considered that not well carbonized structure of the bamboo-cellulose fiber is appropriate for effective activation. The power-spectra images were obtained by 2D-FFT on the TEM images of carbonized samples and then the distributions of interlayer spacing were obtained by integration along rotation-axis of power spectra. The interlayer spacing was estimated to be 0.49 nm (BC-0600), 0.47 nm (BC-0800) and 0.45 nm (BC-1000). The spacing can be considered to be the carbon-carbon interlayer spacing of the basic structural unit (BSU). The specific surface area of 2366 m^2/g is a little bit less than 2543 m^2/g of commercial activated carbon (MSP) which is widely used as the EDLC electrode material. Consequently, the EDLC capacity of the activated carbon derived from bamboo-cellulose fiber was 43 F/g (23 F/cm^3), being almost equal to 44 F/g (22 F/cm^3) of MSP. The present investigation predicts that not only activation process but also carbonization conditions are important for the preparation of nanoporous carbon with large surface area. We should develop in detail about the carbonization conditions of bamboo-cellulose fiber.

Acknowledgements

This research was supported by grants from the Project of the NARO Bio-oriented Technology Research Advancement Institution (Integration research for agriculture and interdisciplinary fields). We express our appreciation to Prof. Morinobu Endo of Shinshu University for his great support and fruitful discussion. We also thank Dr. Noboru Akuzawa of Shinshu University for his kind suggestions.

References

[1] D.K. Tamang, D. Dhakal, S. Gurung, N.P. Sharma, D.G. Shrestha, Bamboo diversity, distribution pattern and its uses in Sikkim (India) Himalaya, Int. J. Sci. Res. Publ. 3 (2013) 1–6.
[2] Japan Special Forest Product Promotion Association, http://nittokusin.jp/wp/wp-content/uploads/2011/09/ef738878d1d3489d1e4333d9375edc88.pdf, (in Japanese).
[3] A. Imaji, M. Ueda, Y. Waguchi, M. Tanaka, A. Uematsu, N. Kasuya, T. Ikeda, Effects of bamboo colonization on water relations of Japanese cedar (Cryptomeria japonica) and Hinoki cypress (Chamaecyparis obtusa), J. Jpn. For. Soc. 95 (2013) 141–146.
[4] Y. Isagi, A. Torii, The range expansion and its mechanism of naturalized bamboo species, J. Sustain. For. 6 (1997) 127–141.
[5] M. Endo, Y.J. Kim, H. Ohta, K. Ishii, T. Inoue, T. Hayashi, Y. Nishimura, T. Maeda, M.S. Dresselhaus, Carbon 40 (2002) 2613–2626.
[6] N. Yamashita, M. Machida, Carbonization of bamboo and consecutive low temperature air activation, Wood Sci. Technol. 45 (2011) 801–808.
[7] S.-H. Lin, L.-Y. Hsu, C.-S. Chou, J.-W. Jhang, P. Wu, Carbonization process of Moso bamboo (*Phyllostachys pubescens*) charcoal and its governing thermodynamics, J. Anal. Pyrol. 107 (2014) 9–16.
[8] P.-H. Huang, J.-W. Jhan, Y.-M. Cheng, H.-H. Cheng, Effects of carbonization parameters of moso-bamboo-based porous charcoal on capturing carbon dioxide, The Sci. World J. 2014 (2014) 1–8 ID 937867.
[9] T.Y. Kim, S.Y. Cho, J.H. Kim, Adsorption characteristics of 2, 4-DNP on bamboo-based activated carbon, Proc. 2015 Int. Conf. Innov. in Chem. and Agri. Eng. (2015) 106–111.
[10] B.O. Evbuomwas, A.S. Abutu, C.P. Ezeh, The effects of carbonization temperature on some physicochemical properties of bamboo based activated carbon by potassium hydroxide (KOH) activation, Greener J. Phys. Sci. 3 (2013) 187–191.
[11] W.N.R.W. Isahak, M.W.M. Hisham, M.A. Yarmo, Highly porous carbon materials from biomass by chemical and carbonization method: a comparison study, J. Chem. 2013 (2013) 1–6 ID 620346.
[12] S. Hirunpraditkoon, N. Tunthong, A. Ruangchai, K. Nuithitikul, Adsorption capacities of activated carbons prepared from bamboo by KOH activation, Int. J. Chem. Mol. Nuclear Mater. Metal. Eng. 5 (2011) 477–481.
[13] T. Tsubota, M. Morita, S. Kamimura, T. Ohno, New approach for syanthesis of activated carbon from bamboo, J. Porous Mater. 23 (2016) 349–355.
[14] H. Chen, D. Liu, Z. Shen, B. Bao, S. Zhao, L. Wu, Functional biomass carbons with hierarchical porous structure for supercapacitor electrode materials, Electrochim. Acta 180 (2015) 241–251.
[15] J.P. Olivier, Improving the models used for calculating the size distriburion of micropore volume of activated carbons from adsorption data, Carbon 36 (1998) 1469–1472.
[16] K.K.H. Choy, J.P. Barford, G. McKay, Production of activated carbon from bamboo scaffolding waste – process design, evaluation and sensitivity analysis, Chem. Eng. J. 109 (2005) 147–165.
[17] S.L. Zuo, S.Y. Gao, X. Yuan, B. Xu, Carbonization mechanism of bamboo (*phyllostachys*) by means of Fourier transform infrared and elemental analysis, J. For. Res. 14 (2003) 75–79.
[18] X. Ma, C. Yuang, X. Liu, Mechanical, microstructure and surface characterization of carbon fibers prepared from cellulose after liquefying and curing, Materials 7 (2014) 75–84.
[19] M. Guigon, A. Oberlin, G. Desarmot, Microtexture and structure of some high-modulus, PAN-base carbon fibres, Fibre Sci. Technol. 20 (1984) 177–198.
[20] K. Oshida, T. Nakazawa, T. Miyazaki, M. Endo, Application of image processing techniques for analysis of nano- and micro-spaces in carbon materials, Synth. Met. 125 (2001) 223–230.
[21] K. Oshida, M. Murata, K. Fujiwara, T. Itaya, T. Yanagisawa, K. Kimura, T. Nakazawa, Y.A. Kim, M. Endo, B.-H. Kim, K.S. Yang, Structural analysis of nano structured carbon by transmission electron microscopy and image processing, Appl. Surf. Sci. 275 (2013) 409–412.
[22] Z.L. Xie, X. Huang, M.-M. Titirici, A. Taubert, Mesoporous graphite nanoflakes via ionothermal carbonization of fructose and their use in dye removal, RSC Adv. 4 (2014) 37423–37430.
[23] R. Vidano, D.B. Fishbach, New lines in the Raman spectra of carbons and graphite, J. Am. Ceram. Soc. 61 (1978) 13–17.
[24] T.C. Chieu, M.S. Dresselhaus, M. Endo, Raman studies of benzene-derived graphite fibers, Phys. Rev. B 26 (1982) 5867.
[25] H. Wang, W. Yu, J. Shi, N. Mao, S. Chen, W. Liu, Biomass derived hierarchical porous carbons as high-performance anodes for sodium-ion batteries, Electrochim. Acta 188 (2016) 103–110.
[26] C. Hu, S. Sedghi, A. Silvestre-Albero, G.G. Andersson, A. h Sharma, P. Pendleton, F. Rodrıguez-Reinoso, K. Kaneko, M.J. Biggs, Raman spectroscopy study of the transformation of the carbonaceous skeleton of a polymer-based nanoporous carbon along the thermal annealing pathway, Carbon 85 (2015) 147–158.
[27] J.M. Dias, M.C.M. Alvim-Ferraz, M.F. Almedia, J. Rivera-utrilla, M. Sanchez-Polo, Waste materials for activated carbon preparation and its use in aqueous-phase treatment: a review, J. Environ. Manage. 85 (2007) 833–846.
[28] J.C. Moreno-Pirajan, L. Giraldo, Study of activated carbons by pyrolysis of mahgnifera indica seed (Mango) in presence of sodium and potassium hydroxide, E-J. Chem. 9 (2012) 780–785.

[29] M.A. Yahya, C.W. Zanariah, C.W. Ngah, M.A. Hashim, Z. Al-Qodah, Preparation of activated carbon from desiccated coconut residue by chemical activation with NaOH, J. Mater. Sci. Res. 5 (2016) 24–31.
[30] M. Thommes, K. Kaneko, A.V. Neimark, J.P. Olivier, F. Rodriguez-Reinoso, J. Rouquerol, K.S.W. Sing, Physisorption of gases, with special reference to the evaluation of surface area and pore size distribution (IUPAC Technical Report), Pure Appl. Chem. 87 (2015) 1051–1069.
[31] M.A. Lillo-Rodenas, J. Juan-Juan, D. Cazorla-Amoros, A. Linares-Solano, About reactions occurring during chemical activation with hydroxides, Carbon 42 (2004) 1371–1375.
[32] D. Hulicova-Jurcakova, M. Kodama, S. Shiraishi, H. Hatori, Z.H. Zhu, G.Q. Lu, Nitrogen-enriched nonporous carbon electrode with extraordinary supercapacitance, Adv. Funct. Mater. 19 (2009) 1800–1809.
[33] K. Hung, C. Masarapu, T. Kao, B. Wei, Wide-temperature range operation supercapacitors from nanostructured activated carbon fibre, J. Power Sources 193 (2009) 944–949.